

# Functionalized Silver Nanoparticle Catalyzed [3+2] Cycloaddition Reaction: Greener Route to Substituted-1,2,3-triazolines

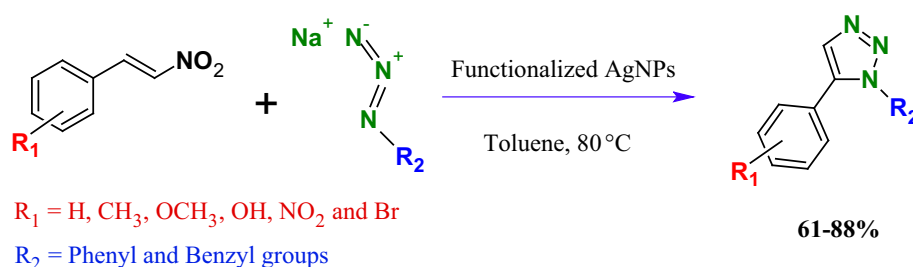
Nanjundaswamy Marishetty Hemmaragala<sup>1</sup> · Heidi Abrahamse<sup>1</sup> · Blassan Plackal Adimuriyil George<sup>1</sup> · Ramesh Gannimani<sup>2</sup> · Patrick Govender<sup>2</sup>

Received: 23 September 2015 / Accepted: 1 November 2015  
© Springer Science+Business Media New York 2015

**Abstract** The [3+2] cycloaddition reaction between nitroolefins and alkyl/aryl azides was studied using functionalized silver nanoparticles (FnAgNPs) of average diameter  $23 \pm 1$  nm as catalyst produced by the plant extract *Protorhus longifolia*. We found FnAgNPs to catalyze the reactions efficiently yielding a series of 1,5-disubstituted-1,2,3-triazolines under mild reaction conditions

with no side products. The catalytic activity of FnAgNPs was compared with naked AgNPs and FnAgNPs found to be very effective. Except solvents, the whole experiments do not require any chemical/reagent which makes the process green.

## Graphical Abstract



**Keywords** Functionalized silver nanoparticles · *Protorhus longifolia* · Catalysis · [3+2]cycloaddition · 1, 5-Disubstituted-1, 2, 3-triazolines

**Electronic supplementary material** The online version of this article (doi:10.1007/s10562-015-1653-x) contains supplementary material, which is available to authorized users.

✉ Nanjundaswamy Marishetty Hemmaragala  
nswamyorg@gmail.com

<sup>1</sup> Laser Research Centre, Faculty of Health Sciences,  
University of Johannesburg,  
P. O. Box 17011, Doornfontein 2028, South Africa

<sup>2</sup> School of Life Sciences, Westville Campus, University of  
KwaZulu-Natal, Durban 4000, South Africa

## 1 Introduction

The use of soluble form of gold started in 290 AD for artwork purposes [1]. However, researchers are attracted to explore the synthesis and use of gold nanoparticles after Michael Faraday's experiment on the reduction of chloroaurate salts by phosphorous in  $\text{CS}_2$  to obtain deep red colloidal solutions of gold [2]. Since then, thousands of research articles reported the synthesis, properties and assembly of nanoparticles employing numerous methodologies and materials [1]. More recently, nanomaterials

technologies found new applications in all possible areas of human needs and the use of nanomaterials to catalyze organic reactions is one of the most important claims [3]. Consequently the synthesis of a plethora of organic molecules by homogeneous and heterogeneous catalysis under mild reaction conditions, easy work-up procedures and with less polluting processes has been realized [4]. In particular, silver and gold nanoparticles become an important tool for chemists and biologists owing to their wide spectra of applications in constructing bio-molecules and even as prime agents for drug delivery [5, 6]. The size and the shape of silver and gold nanoparticles can be varied to express various colors by surface plasmon absorption leading to a plethora of diverse biological and chemical applications [7]. Therefore, the synthesis of Ag and Au nanoparticles and the discovery of their applications is critical and current interest.

In this context, numerous methods have been established for the production of Ag and Au nanoparticles. However, chemical methods suffer for the use of toxic reagents that can be also adsorbed onto the surface of nanoparticles [8]. Use of plant extracts for the extracellular synthesis of silver nanoparticles in a top-down reduction fashion is very interesting and has been extensively studied [9]. These methods comprise less cumbersome procedures and are considered to be highly convenient due to milder reaction conditions, reproducibility and easy availability of plant materials. Plant extract mediated silver nanoparticles very often have unique chemical and biological properties and are interesting as catalysis to construct bioactive compounds [10]. The phytochemicals present in the plant extracts reduces the metal ions to produce nanoparticles and often at the same time the functionalization of the surface of nanoparticles can occur [11]. This functionalization is responsible for the increase of the biocompatibility of nanoparticles and the functionalized nanoparticles are also attributed to be stable colloidal form due to steric repulsion between the organic moieties. The influence of chemical composition of plant extract significantly affects the size and shape of the nanoparticles and the catalytic properties as well [12]. Therefore there is an increasing interest in exploring plant extracts for the production of silver nanoparticles and to study their shape, size and the catalytic activities. Current reports on the synthesis of silver and gold nanoparticles using plant extracts include peel of mango [13], lemon [14], Satsuma mandarin [15], root extract of *Zingiber officinale* [16], sea weed *Chaetomorpha linum* [17], flower extracts of *Gnidia glauca* [18], *Nyctanthes arbortristis* [19], *Carthamus tinctorius L* [20], leaf extracts of *Gliricidia sepium* [21], seed extracts of *Abelmoschus esculentus* [22], and *Acacia farnesiana* [23].

On the other hand, heterocyclic chemistry is playing major role in synthetic organic chemistry especially as

heterocyclic compounds are efficient drug candidates. Interestingly, more than 90 percent of new drug molecules, drug intermediates and other bio-molecules are heterocycles [24]. 1,2,3-Triazoles are an important class of heterocycles and are widely used in the construction of promising novel bio-molecules [25]. Indeed, the derivatives of 1,2,3-triazoles are known to possess antifungal [26], antiviral [27] antibacterial [28] and antitumor activities [29]. For example, analogues of zanamivir embedding the 1,2,3-triazole nucleus has been successfully screened as anti-HIV [30]. Additionally, cyclopentenyl carbocyclic nucleosides, conjugated with 1,2,3-triazoles has been reported as potent antiviral agent against orthopoxviruses and severe acute respiratory syndrome [31]. 3-Arylethyl-triazolyl ribonucleosides are shown to possess potent anticancer activity on the drug-resistant pancreatic cancer cell line MiaPaca-2 [32]. Phokodylo et al. recently reported the conjugation of 1,2,3-triazole with oxadiazoles and thiazoles to afford compounds that are active against melanoma, colon and breast cancer [33]. For these reasons, the scientific community showed an increasing interest in search of easy routes for the synthesis of 1,2,3-triazoles [34]. There are three major methods for the synthesis of 1,2,3-triazole moiety, all involving a [3+2] cycloaddition reaction of azides with alkynes, nitriles and nitro olefins, respectively. These reactions have been carried out employing a number of metal catalysts and toxic reagents under various reaction conditions and still there is a scope in developing easy and environmentally friendly process to obtain 1,2,3-triazoles [35].

## 2 Results and Discussion

In continuation of our research on the synthesis, functionalization, and use of nanoparticles, [36, 37], herein we report the synthesis of 1,5-disubstituted-1,2,3-triazoles via [3+2] cycloaddition reaction of nitroolefins and azides. The reactions have been catalyzed by functionalized silver nanoparticles obtained by the plant source *Protorhus longifolia*. *Protorhus longifolia* belongs to the *Anacardiaceae* family which is widely distributed throughout South Africa [38]. The bark and leaves of *Protorhus longifolia* are used in traditional medicine to treat hemiplegic paralysis, heart burn and stomach bleed [39]. We were interested in using the aqueous seed extract of these species as a reducing agent for the production of silver nanoparticles and to study their catalytic activity in [3+2] cycloaddition reaction between nitroolefins and azides for the syntheses of substituted 1,2,3-triazoles. In a typical experiment, 2 ml of plant extract was added to 25 ml of sterile 1 mM silver nitrate solution and incubated with continuous stirring on the rotary shaker at 120 rpm for 24 h

at 30 °C. After the addition of the seed extract, the silver nitrate solution changed from colorless to brown color indicating the reduction of  $\text{Ag}^+$ . Both the intensity in color of the reaction mixture and absorbance increased with the time as the reaction proceeded. The progress of the reaction for the formation of AgNPs was monitored by the periodical measurement of UV absorbance at 400–500 nm, Fig. 1. Upon the completion of reaction, the colloidal solution was centrifuged at 4000 rpm for 20 min and the residue washed with distilled water to remove unreacted material. The infra-red spectrum of the obtained silver nanoparticles revealed the presence of organic functional groups on the surface of silver nanoparticles to form a capping agent. Figure 2 shows the main absorptions at 3258, 1629, 1514, 1055  $\text{cm}^{-1}$  in IR spectroscopy. The broad peak at 3258  $\text{cm}^{-1}$  indicates strong stretching vibrations of -OH functional groups and at 1055  $\text{cm}^{-1}$  for ether linkages or -C-O- groups. The absorbance at 1629  $\text{cm}^{-1}$  might be the stretching vibrations of alkene groups -C=C-. Additionally, the observed peaks can also be attributed to polyols such as flavones, terpenoids and polysaccharides present in the seed extract. The functionalized silver nanoparticles have been thoroughly characterized by scanning electron microscopy and transmission electron microscopy (TEM) as depicted in Fig. 3. The AgNPs arising from the reaction mixture were repeatedly centrifuged and re-dispersed in sterile distilled water prior to SEM and TEM analysis to remove any unreacted plant material and metal ions. SEM analysis confirmed that particles are of a nano-size. The spherical shape of the nanoparticles is shown in the SEM images. The EDX analysis confirmed that the particles were composed of element silver. TEM analysis showed that silver nanoparticles were poly-dispersed and predominantly spherical or

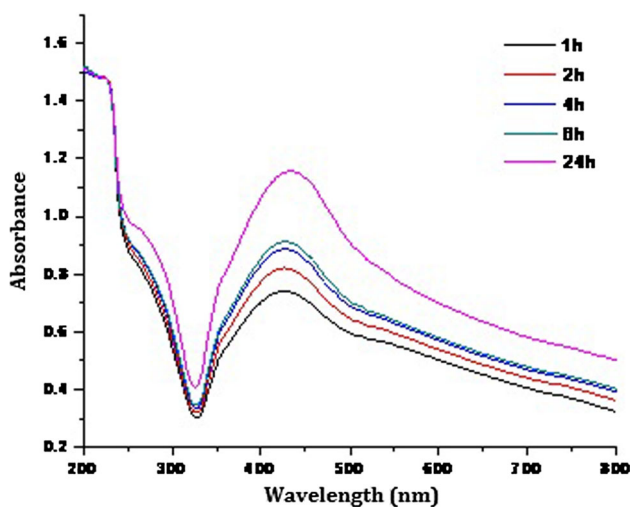


Fig. 1 Monitoring the synthesis of AgNPs: UV-Vis spectra

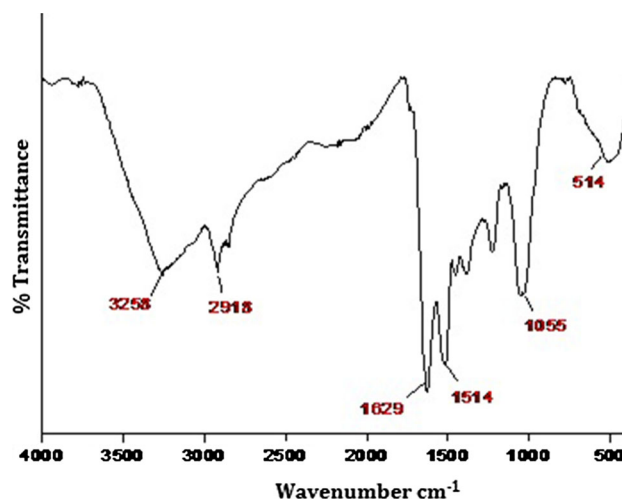
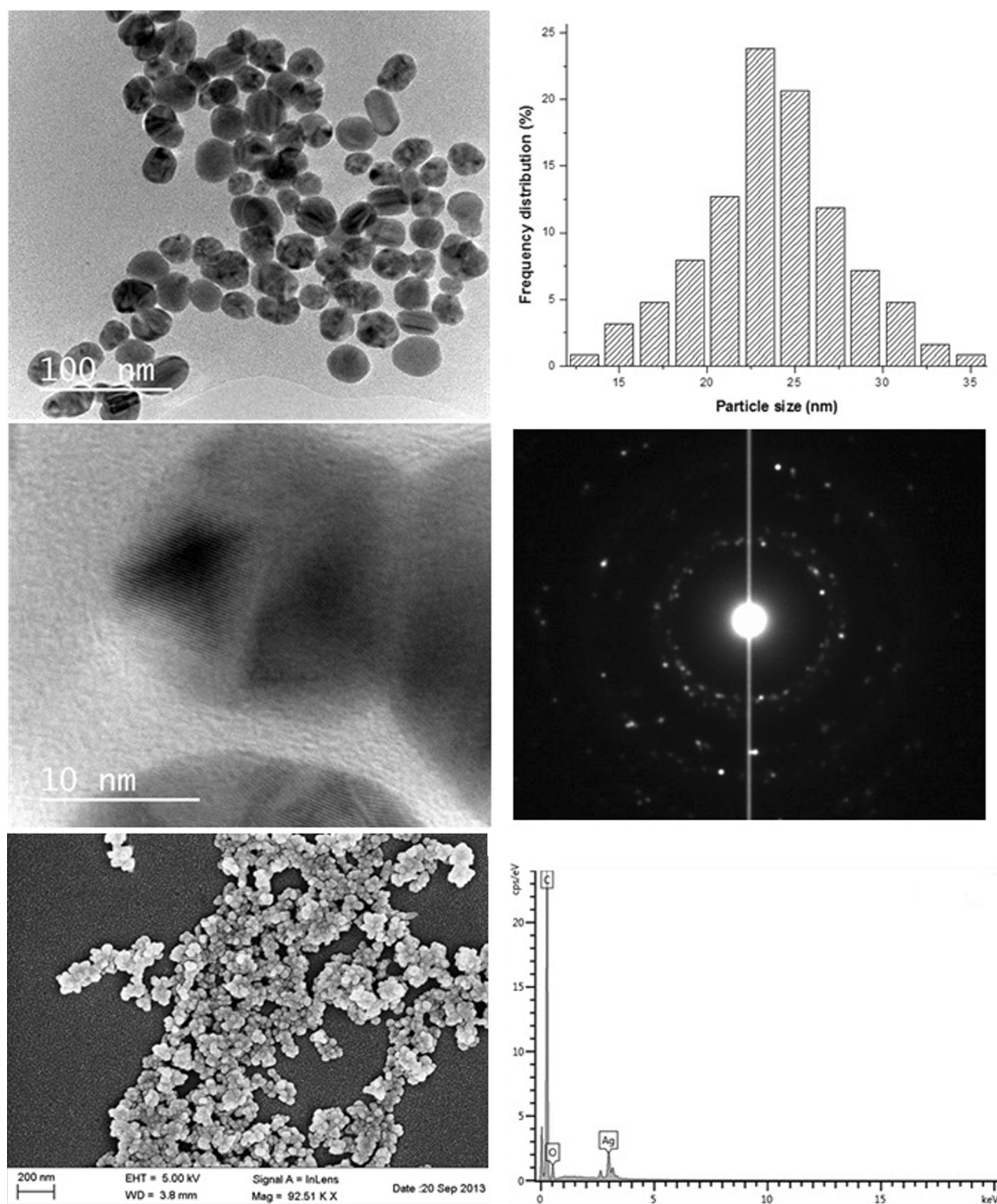


Fig. 2 FTIR spectra of functionalized AgNPs

polyhedral in shape. The majority of the silver nanoparticles were  $23 \pm 1$  nm in size and the embedded figure clearly shows the morphology of silver nanoparticles. The selected area diffraction pattern clearly indicated that the AgNPs formed by the reduction of metal ions by the seed extract are polycrystalline in nature with clear lattice fringes, characteristic of crystalline nature of the obtained nanoparticle.

After characterization of the AgNps, we were excited to know their efficiency as catalyst for the [3+2] cycloaddition reactions between nitroolefins and azides for the synthesis of 1,5-disubstituted-1,2,3-triazolines. Thus, a solution of (2-nitroethyl)benzene (**1a**) (150 mg, 1.0 mmol) in toluene (5 mL) was prepared in a 10 mL round bottomed flask fitted with a magnetic stirrer. Then, phenyl azide (**2a**) (155 mg, 1.3 equiv.) and AgNPs (100 mg) were added and the reaction mixture heated at 80 °C. The reaction was monitored via TLC by the disappearance of starting material (2-nitroethyl) benzene. Upon completion of the reaction, the reaction flask was cooled, and the mixture was centrifuged. The residue (AgNPs) was separated by simple filtration. The filtrate was evaporated off under reduced pressure to afford the crude product which was purified by column chromatography over silica gel, using ethyl acetate/hexane (1.5: 8.5) as eluent, to afford 118 mg of solid 1,5-diphenyl-1*H*-1,2,3-triazole (**3a**) in 61 % yield. Further, the effect of catalyst loading, reaction times and the efficacy of functionalized AgNps over naked AgNP were studied and the results are shown in Table 1. 80 mg of functionalized AgNps are necessary and sufficient to catalyze the reaction and to afford the maximum reaction yield. Moreover, functionalized AgNPs are more efficient catalysts than naked AgNPs. Triggered by these results, we wanted to extend the suitability of the method to the reactions of different substituted nitroolefins bearing



**Fig. 3** Clockwise from *top left* **a** HRTEM micrograph; **b** Histogram, SAED pattern; Lattice fringes; **c** SAED pattern; **d** EDX pattern; **e** SEM morphology and **f** Lattice fringes

**Table 1** Catalytic loading of functionalized AgNPs and comparison of the results with naked AgNPs for the reaction between (2-nitroethenyl)benzene and phenyl azide

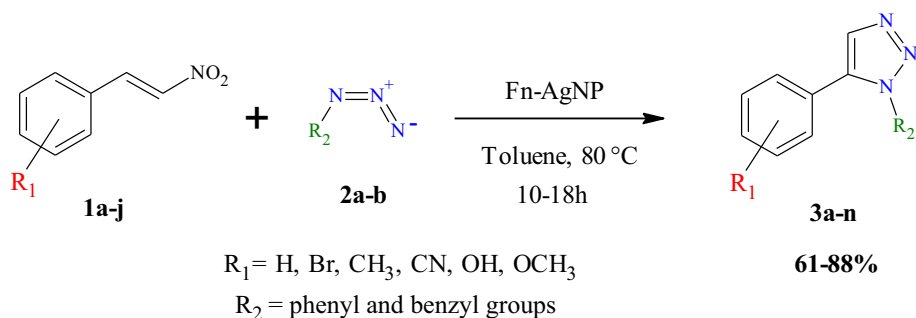
| Entry | Catalyst (mg) |             | Time | Yields (%)  |         |
|-------|---------------|-------------|------|-------------|---------|
|       | Naked AgNP    | Fn-AgNP (h) |      | Naked AgNP  | Fn-AgNP |
| 1     | 10            | 10          | 18   | Trace       | Trace   |
| 2     | 20            | 20          | 18   | Trace       | 32      |
| 3     | 30            | 30          | 18   | <5 % on TLC | 41      |
| 4     | 40            | 40          | 18   | <5 % on TLC | 57      |
| 5     | 50            | 50          | 18   | 12          | 59      |
| 6     | 80            | 80          | 18   | 18          | 63      |
| 7     | 100           | 100         | 18   | 25          | 65      |
| 8     | 80            | 80          | 12   | 15          | 61      |
| 9     | 80            | 80          | 10   | 12          | 55      |

respectively methoxy, nitro, bromo, chloro, tolyl, hydroxyl and cyano groups with phenyl and benzyl azides to get the corresponding 1,5-disubstituted-1,2,3-triazoles, Scheme 1 and Table 2. Table 2, entry 1 reports the best comprise between catalyst loading, reaction time and yield achieved during the screening reported in Table 1 (entry 8). The reaction works well with phenyl azide (**2a**) and aryl nitroolefins **1b-d** bearing both ED or EW groups on the aryl moiety yielding the corresponding triazoles **3b-d** in 64–75 % yield (entries 2–4). A similar result (**3e**, 62 % yield) was obtained working with (*E*)-2-(2-nitrovinyl)thiophene (**1e**), entry 5. Moreover, Fn-AgNP efficiently catalyzed the reaction of nitroolefins **1** with benzyl azide (**2b**) entries 6–14. Thus, model nitroolefin **1a** as well as substituted nitroolefins **1b, c, f, g**, nitrovinylthiophene **1e** afforded the corresponding triazoles **3f-j, n** in 65–88 % yield, entries 6–10, 14. Good results were obtained also with ortho-substituted nitroolefins **1h, j** (entries 11, 13; **3k, 3m**; 86 %) whereas worst yield (**3l**, 24 %) were observed with (*E*)-4-(2-nitrovinyl)benzotrile **1i**. In this latter case, a mixture of products namely the 4-(1-benzyl-1*H*-1,2,3-triazol-5-yl) benzotrile and 4-(1-benzyl-1*H*-1,2,3-triazol-5-yl)[5-phenyl-1*H*-1,2,3,4-tetrazole], were expected, but only 4-(1-benzyl-1*H*-1,2,3-triazol-5-yl) benzotrile in 24 % yield was isolated after 18 h.

### 3 Experimental Section

#### 3.1 Materials and Methods

Silver nitrate, ( $\text{AgNO}_3$ ) was of analytical grade reagents purchased from Merck Germany. 1 % JIK bleach was purchased from Reckitt Benckiser, South Africa. Seeds of *Protorhus longifolia* were collected from Westville campus, University of KwaZulu-Natal (GPS co-ordinates  $-29.817897, 30.942771$ ). UV-Vis measurements have been studied at room temperature as function of time using Specord 210, Analytikjena spectrometer. 1 mM  $\text{AgNO}_3$  solution was used as the blank. FTIR-ATR Spectroscopy measurements have been recorded by making pellets of functionalized nanoparticles. Scanning Electron Microscopy for morphological studies of the synthesized AgNPs was carried out using scanning electron microscopy (FEGSEM ZEISS ULTRAPLUS). Samples prepared by adding a drop of sonicated nanoparticle solution over the carbon tape glued over metal stub. The samples thus obtained were coated with carbon and observed at 10000 X magnification. The energy dispersive X-ray analysis (EDX) was done at 20 kV using AZTEC software for the analysis. TEM obtained after sonication for 15 min to disrupt any possible aggregate. A small amount of this sonicated

**Scheme 1** Synthesis of substituted-1,2,3-triazolines from nitroolefins and azides catalyzed by functionalized AgNP

**Table 2** Synthesis of 1,5-disubstituted-1,2,3-triazolines by the reaction of nitroolefins and azides catalyzed by Functionalized AgNPs

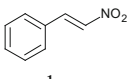
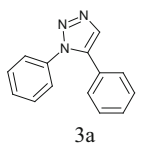
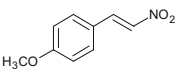
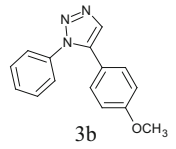
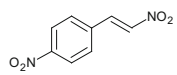
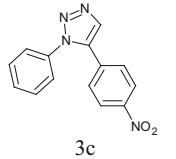
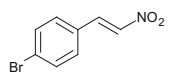
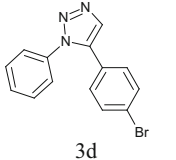
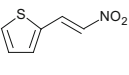
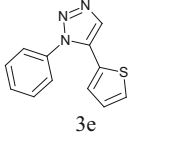
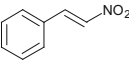
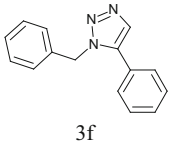
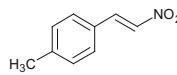
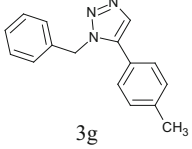
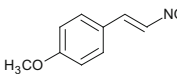
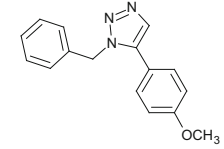
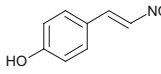
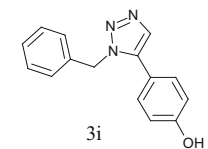
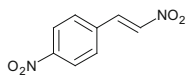
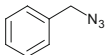
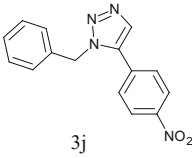
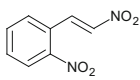
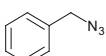
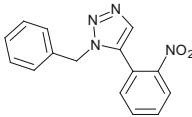
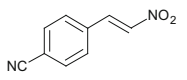
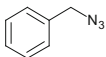
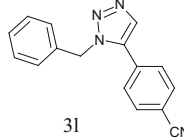
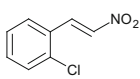
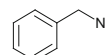
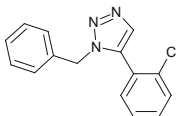
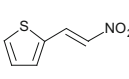
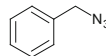
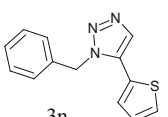
| Entry | Nitroolefin<br>(1a-j)   | Azide<br>2a, 2b   | Reaction<br>time (h) | Product<br>(3a-n)  | Yield(%) |
|-------|---|---|----------------------|--|----------|
| 1     | <br>1a   | <br>2a   | 12                   | <br>3a   | 61       |
| 2     | <br>1b   | <br>2a   | 13                   | <br>3b   | 64       |
| 3     | <br>1c   | <br>2a   | 10                   | <br>3c   | 72       |
| 4     | <br>1d   | <br>2a   | 18                   | <br>3d   | 75       |
| 5     | <br>1e | <br>2a | 13                   | <br>3e | 62       |
| 6     | <br>1a | <br>2b | 18                   | <br>3f | 80       |
| 7     | <br>1f | <br>2b | 18                   | <br>3g | 76       |
| 8     | <br>1b | <br>2b | 18                   | <br>3h | 74       |
| 9     | <br>1g | <br>2b | 18                   | <br>3i | 65       |

Table 2 continued

| Entry | Nitroolefin<br>(1a-j)  | Azide<br>2a, 2b  | Reaction<br>time (h) | Product<br>(3a-n)   | Yield(%) |
|-------|--|--|----------------------|---|----------|
| 10    | <br>1c  |   | 18                   | <br>3j  | 88       |
| 11    | <br>1h  |   | 18                   | <br>3k  | 86       |
| 12    | <br>1i  |   | 18                   | <br>3l  | 24       |
| 13    | <br>1j  |   | 12                   | <br>3m  | 86       |
| 14    | <br>1e |  | 12                   | <br>3n | 68       |

suspension was placed on carbon coated copper grid and dried under infrared light for solvent evaporation. High-resolution TEM images were obtained on JEOL TEM model no 2100 operating at accelerating voltage of 200 kV and 0.23 nm resolution. Nitroolefins were synthesized according to a previous procedure. All solvents were of analytical grade and purified wherever necessary according to standard procedures prior to use. TLCs were run on pre-coated silica gel on aluminium plates obtained from Whatmann Inc. All reactions were performed at 80 °C. Büchi B-540 apparatus was used to obtain the melting points of all solid compounds. Bruker- TENSOR-FTIR instrument was used to record IR spectroscopy. <sup>1</sup>H NMR and <sup>13</sup>C NMR spectra were recorded on Bruker Avance 400 and 100 MHz spectrometer respectively, chemical shifts were reported in (ppm) with TMS as internal standard. Yields of pure isolated compounds after column chromatography (70–230) mesh silica gel) are reported.

### 3.2 General Procedure for Fn-AgNP Catalyzed Synthesis of 1,5-Disubstituted-1,2,3-triazoles 3a–n

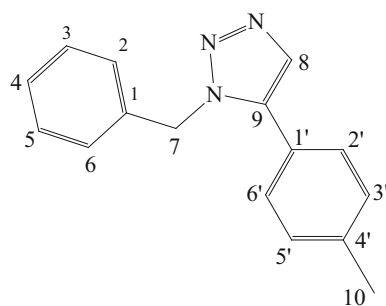
A solution of nitroolefins 1a–j (1.0 mmol) in toluene (5 mL) was prepared in 10 mL round bottomed flask fitted

with a magnetic stirrer. Then, azides (**2a,b**) (1.3 equiv.) and AgNPs (80 mg) were added and the reaction mixture heated at 80 °C. The reaction was monitored via TLC by the disappearance of starting nitroolefins. Upon completion of the reaction, the reaction flask was cooled, and the mixture was centrifuged. The residue (AgNPs) was separated by simple filtration. The filtrate was evaporated off under reduced pressure to afford the crude products which were purified by column chromatography over silica gel, using ethyl acetate/hexane (1.5: 8.5) as eluent. The corresponding triazoles 3a–n were isolated, see Table 2 for details.

## 4 Conclusion

In summary, a benign procedure for the syntheses of 1,5-diphenyl-1*H*-1,2,3-triazolines employing functionalized silver nanoparticles produced in green way has been proposed. Except the use of solvents, the entire process does not involve any chemical reagents neither to produce the nanoparticles nor to catalyze the reactions. Therefore we believe the procedure would be of general use for synthetic chemists.

## 4.1 Spectroscopic Characterization Data



Example for atom numbering

### 4.1.1 1,5-Diphenyl-1H-1,2,3-triazole (**3a**) Yield

61 %; white solid, mp: 113–114 °C (lit. 113–114 °C)<sup>22</sup>; <sup>1</sup>H NMR (400 MHz, CDCl<sub>3</sub>): δ 7.87 (s, 1H, triazolyl-H), 7.47–7.41 (m, 3H, Ar-H), 7.40–7.32 (m, 5H, Ar-H), 7.24–7.21 (m, 2H, Ar-H) ppm; <sup>13</sup>C NMR (100 MHz, CDCl<sub>3</sub>) δ 137.7 (triazolyl-C8), 136.6 (C1), 133.4 (triazolyl-C7), 129.4 (C2', C6'), 129.2 (C3, C5), 128.9 (C3', C5'), 128.6 (C4, C4'), 126.8 (C1'), 125.2 (C2, C6) ppm.

### 4.1.2 Methyl 4-(1-Phenyl-1H-1,2,3-triazol-5-yl)phenyl Ether (**3b**)

Yield 64 %; Yellow oil [22]; <sup>1</sup>H NMR (400 MHz, CDCl<sub>3</sub>) δ 7.79 (s, 1H, triazolyl-H), 7.45–7.35 (m, 5H, Ar-H), 7.18–7.12 (m, 2H, Ar-H), 6.87–6.84 (m, 2H, Ar-H), 3.80 (s, 3H, OCH<sub>3</sub>); <sup>13</sup>C NMR (100 MHz, CDCl<sub>3</sub>): δ 161.2 (triazolyl-C8), 137.5 (C1), 136.4 (C4'), 133.1 (triazolyl-C7), 130.0 (C3', C5'), 129.4 (C3, C5), 129.2 (C2', C6'), 125.1 (C2, C6), 119.0 (C1'), 114.2 (C4), 55.1 (OCH<sub>3</sub>).

### 4.1.3 5-(4-Nitrophenyl)-1-phenyl-1H-1,2,3-triazole (**3c**)

Yield 72 %; Yellow solid, mp: 144–145 °C (144–145 °C) [23]; <sup>1</sup>H NMR (400 MHz, CDCl<sub>3</sub>): δ 8.22–8.19 (m, 2H, Ar-H), 7.97 (s, 1H, triazolyl-H), 7.51–7.43 (m, 3H, Ar-H), 7.45–7.40 (m, 2H, Ar-H), 7.38–7.32 (m, 2H, Ar-H); <sup>13</sup>C NMR (100 MHz, CDCl<sub>3</sub>): δ 147.7 (C4'), 135.5 (triazolyl-C7), 134.2 (C1), 133.1 (triazolyl-C8), 129.8 (C1'), 129.6 (C3, C5), 129.3 (C2', C6'), 125.4 (C3', C5'), 124.4 (C4), 124.1 (C2, C6).

### 4.1.4 5-(4-Bromophenyl)-1-phenyl-1H-1,2,3-triazole (**3d**)

Yield 75 %; Yellow solid, mp: 150–151 °C (149–151 °C) [17]; <sup>1</sup>H NMR (400 MHz, CDCl<sub>3</sub>): δ 7.86 (s, 1H, triazolyl-H), 7.51–7.43 (m, 5H, Ar-H), 7.37–7.31 (m, 2H, Ar-H),

7.14–7.07 (m, 2H, Ar-H); <sup>13</sup>C NMR (100 MHz, CDCl<sub>3</sub>) δ: 136.4 (triazolyl-C8), 133.3 (C1), 132.6 (triazolyl-C7), 132.3 (C3', C5'), 130.2 (C1'), 129.8 (C3, C5), 129.5 (C2', C6'), 125.7 (C4), 125.2 (C2, C6), 123.4 (C4').

### 4.1.5 1-Phenyl-5-(2-thienyl)-1H-1,2,3-triazole (**3e**)

Yield 62 %; Brown oil [17]; <sup>1</sup>H NMR (400 MHz, CDCl<sub>3</sub>): δ 7.89 (s, 1H, triazolyl-H), 7.55–7.48 (m, 3H, Ar-H), 7.49–7.40 (m, 2H, Ar-H), 7.36 (d, *J* = 5.1 Hz, 1H, thienyl-H), 7.03–6.95 (m, 1H, thienyl-H), 6.94 (d, *J* = 3.7 Hz, 1H, thienyl-H); <sup>13</sup>C NMR (100 MHz, CDCl<sub>3</sub>): δ 136.5 (C1), 133.2 (triazolyl-C8), 132.4 (thienyl-C9), 130.1 (triazolyl-C7), 129.5 (C3, C5), 128.2 (thienyl-C11), 127.7 (thienyl-C10), 127.7 (thienyl-C12), 127.1 (C4), 126.3 (C2, C6).

### 4.1.6 1-Benzyl-5-phenyl-1H-1,2,3-triazole (**3f**)

Yield 80 %; White solid, mp: 72–73 °C (72–74 °C) [22]; <sup>1</sup>H NMR (400 MHz, CDCl<sub>3</sub>): δ 7.77 (s, 1H, triazolyl-H), 7.46–7.33 (m, 3H, Ar-H), 7.34–7.26 (m, 5H, Ar-H), 7.12–7.01 (m, 2H, Ar-H), 5.58 (s, 2H, benzyl-CH<sub>2</sub>); <sup>13</sup>C NMR (100 MHz, CDCl<sub>3</sub>): δ 138.1 (triazolyl-C9), 135.3 (triazolyl-C8), 133.2 (C1), 129.7 (C2', C6'), 129.0 (C3', C5'), 128.8 (C3, C5), 128.3 (C4), 128.1 (C4'), 127.1 (C2, C6), 126.8 (C1'), 52.1 (benzyl-C7).

### 4.1.7 1-Benzyl-5-(4-methylphenyl)-1H-1,2,3-triazole (**3g**)

Yield 76 %; Colourless oil [22]; <sup>1</sup>H NMR (400 MHz, CDCl<sub>3</sub>): δ 7.73 (s, 1H, triazolyl-H), 7.31–7.27 (m, 3H, Ar-H), 7.22 (d, *J* = 8.0 Hz, 2H, Ar-H), 7.14 (d, *J* = 8.1 Hz, 2H, Ar-H), 7.05–7.02 (m, 2H, Ar-H), 5.54 (s, 2H, benzyl-CH<sub>2</sub>), 2.40 (s, 3H, Ar-CH<sub>3</sub>); <sup>13</sup>C NMR (100 MHz, CDCl<sub>3</sub>): δ 139.5 (triazolyl-C9), 138.2 (C4'), 135.7 (triazolyl-C8), 133.2 (C1), 129.7 (C3', C5'), 128.8 (C3, C5), 128.8 (C2', C6'), 128.1 (C2, C6), 127.2 (C4), 123.9 (C1'), 51.6 (benzyl-C), 21.3 (CH<sub>3</sub>).

### 4.1.8 1-Benzyl-5-(4-methoxyphenyl)-1H-1,2,3-triazole (**3h**)

Yield 74 %; Pale yellow oil [22]; <sup>1</sup>H NMR (400 MHz, CDCl<sub>3</sub>): δ 7.71 (s, 1H, triazolyl-H), 7.32–7.28 (m, 3H, Ar-H), 7.16–7.13 (m, 2H, Ar-H), 7.08–7.05 (m, 2H, Ar-H), 6.95–6.91 (m, 2H, Ar-H), 5.54 (s, 2H, benzyl-CH<sub>2</sub>), 3.83 (s, 3H, Ar-OCH<sub>3</sub>); <sup>13</sup>C NMR (100 MHz, CDCl<sub>3</sub>): δ 160.6 (C4'), 137.9 (triazolyl-C9), 135.6 (triazolyl-C8), 133.1 (C1), 130.3 (C2', C6'), 128.8 (C3, C5), 128.1 (C4), 127.3 (C2, C6), 118.9 (C1'), 114.4 (C3', C5'), 55.8 (OCH<sub>3</sub>), 51.3 (benzyl-C).

#### 4.1.9 4-(1-Benzyl-1H-1,2,3-triazol-5-yl)phenol (**3i**)

Yield 65 %; Yellow solid, mp: 179–181 °C (179–181 °C) [17]; <sup>1</sup>H NMR (400 MHz, CDCl<sub>3</sub>): δ 7.70 (s, 1H, triazolyl-H), 7.41–7.23 (m, 4H, Ar-H), 7.12–7.09 (m, 3H, Ar-H), 6.97–6.83 (m, 2H, Ar-H), 5.53 (s, 2H, benzyl-CH<sub>2</sub>), 5.30 (s, 1H, Ar-OH); <sup>13</sup>C NMR (100 MHz, CDCl<sub>3</sub>): δ 157.5 (C4'), 138.3 (triazolyl-C9), 135.3 (triazolyl-C8), 132.8 (C1), 130.4 (C2', C6'), 128.9 (C3, C5), 128.2 (C4), 127.4 (C2, C6), 118.4 (C1'), 116.1 (C3', C5'), 51.5 (benzyl-C).

#### 4.1.10 1-Benzyl-5-(4-nitrophenyl)-1H-1,2,3-triazole (**3j**)

Yield 88 %; Yellow solid, mp: 96–99 °C (96–99 °C) [24]; <sup>1</sup>H NMR (400 MHz, CDCl<sub>3</sub>): δ 8.25 (d, *J* = 8.7 Hz, 2H, Ar-H), 7.81 (s, 1H, triazolyl-H), 7.43 (d, *J* = 8.8 Hz, 2H, Ar-H), 7.30–7.28 (m, 3H, Ar-H), 7.10–7.03 (m, 2H, Ar-H), 5.61 (s, 2H, benzyl-CH<sub>2</sub>); <sup>13</sup>C NMR (100 MHz, CDCl<sub>3</sub>): δ 148.3 (C4'), 134.6 (triazolyl-C9), 134.1 (triazolyl-C8), 131.2 (C1), 129.7 (C2', C6'), 129.0 (C3, C5), 128.6 (C1'), 127.6 (C4), 126.9 (C3', C5'), 124.1 (C2, C6), 52.5 (benzyl-C).

#### 4.1.11 1-Benzyl-5-(2-nitrophenyl)-1H-1,2,3-triazole (**3k**)

Yield 86 %; Yellow solid, mp: 149–151 °C (149–151 °C) [25]; <sup>1</sup>H NMR (400 MHz, CDCl<sub>3</sub>): δ 8.12 – 8.05 (m, 1H, Ar-H), 7.67–7.60 (m, 2H, Ar-H), 7.56–7.51 (m, 1H, triazolyl-H), 7.22–7.17 (m, 5H, Ar-H), 7.02 (dd, *J* = 7.6, 1.3 Hz, 1H, Ar-H), 5.42 (s, 2H, benzyl-CH<sub>2</sub>); <sup>13</sup>C NMR (100 MHz, CDCl<sub>3</sub>): δ 148.4 (C4'), 134.2 (triazolyl-C9), 133.7 (triazolyl-C8), 133.4 (C1), 133.2 (C4'), 133.1 (C4), 131.1 (C3'), 128.7 (C3, C5), 128.4 (C2, C6), 127.7 (C6'), 124.9 (C5'), 122.3 (C1'), 52.6 (benzyl-C).

#### 4.1.12 4-(1-Benzyl-1H-1,2,3-triazol-5-yl)Benzonitrile (**3l**)

Yield 24 %; Yellow solid, mp: 85–86 °C (84–86 °C) [17]; <sup>1</sup>H NMR (400 MHz, CDCl<sub>3</sub>): δ 7.78 (s, 1H, triazolyl-H), 7.74–7.66 (m, 2H, Ar-H), 7.39–7.33 (m, 2H, Ar-H), 7.31–7.25 (m, 3H, Ar-H), 7.06–6.95 (m, 2H, Ar-H), 5.56 (s, 2H, benzyl-CH<sub>2</sub>); <sup>13</sup>C NMR (100 MHz, CDCl<sub>3</sub>): δ 136.3 (triazolyl-C9), 134.9 (triazolyl-C8), 133.8 (C1), 132.7 (C3', C5'), 131.4 (C4), 129.5 (C3, C5), 129.2 (C2, C6), 128.3 (C1'), 126.8 (C2, C6), 117.7 (C ≡ N), 113.2 (C4'), 52.5 (benzyl-C).

#### 4.1.13 1-Benzyl-5-(2-chlorophenyl)-1H-1,2,3-triazole (**3m**)

Yield 86 %; White solid, mp: 58–59 °C (58–60 °C) [17]; <sup>1</sup>H NMR (400 MHz, CDCl<sub>3</sub>): δ 7.71 (s, 1H, triazolyl-H), 7.49 (dd, *J* = 8.1, 1.0 Hz, 1H, Ar-H), 7.41–7.38 (m, 1H,

Ar-H), 7.28–7.16 (m, 4H, Ar-H), 7.01 (dd, *J* = 7.6, 1.6 Hz, 1H, Ar-H), 6.95 (dd, *J* = 7.5, 1.7 Hz, 2H, Ar-H), 5.44 (s, 2H, benzyl-CH<sub>2</sub>); <sup>13</sup>C NMR (100 MHz, CDCl<sub>3</sub>): δ 134.8 (triazolyl-C9), 134.8 (triazolyl-C8), 134.4 (C1), 134.3 (C2'), 132.0 (C1'), 131.2 (C4'), 129.9 (C4), 128.6 (C3, C5), 128.2 (C3'), 127.7 (C2, C6), 126.9 (C6'), 126.4 (C5'), 52.5 (benzyl-C).

#### 4.1.14 1-Benzyl-5-(2-thienyl)-1H-1,2,3-triazole (**3n**)

Yield 68 %; Yellow solid, mp: 78–79 °C (77–79 °C) [17]; <sup>1</sup>H NMR (400 MHz, CDCl<sub>3</sub>): δ 7.81 (s, 1H, triazolyl-H), 7.44 (dd, *J* = 5.1, 1.2 Hz, 1H, thienyl-H), 7.34–7.26 (m, 3H, Ar-H), 7.13–7.05 (m, 3H, Ar-H, 2H, thienyl-H, 1H), 7.02 (dd, *J* = 3.6, 1.2 Hz, 1H, thienyl-H), 5.66 (s, 2H, benzyl-CH<sub>2</sub>); <sup>13</sup>C NMR (100 MHz, CDCl<sub>3</sub>): δ 135.2 (triazolyl-C9), 133.7 (C1), 131.9 (thienyl-C10), 128.9 (C3, C5), 128.4 (triazolyl-C8), 128.2 (C4), 128.1 (thienyl-C12), 127.9 (thienyl-C11), 126.8 (C2, C6), 126.4 (thienyl-C13), 52.3 (benzyl-C).

## References

- Satoshi H, Nick S (2013) Introduction to Nanoparticles. In: Microwaves in Nanoparticle Synthesis, 1st edn. Wiley-VCH Verlag GmbH & Co. KGaA, Weinheim, pp 1–24
- Faraday M (1857) Philos Trans R Soc Lond 147:145
- Bhosale MA, Bhanage BM (2015) Curr org chem 19:708
- Ranu BC, Chattopadhyay K, Adak L, Saha A, Bhadra S, Dey R, Saha D (2009) Pure Appl Chem 81:2337
- Abbiati G, Rossi E (2014) Beilstein J Org Chem 10:481
- Adeyemi OS, Sulaiman FA (2015) J Biomed Res 29:145
- Kretschmer F, Muhlig S, Hoepfner S, Winter A, Hager MD, Rockstuhl C, Pertsch T, Schubert US (2014) Part Part Syst Charact 31:721
- Yahyaei B, Arabzadeh S, Pourali P (2014) J Pure Appl Microbio 8:4495
- Banerjee S, Satapathy M, Mukhopadhyay A, Das P (2014) Bioprocess Bioprocess 1:1
- Ahmed S, Ahmad M, Swami BL, Ikram S (2015) J Adv Res. doi:10.1016/j.jare.2015.02.007
- Gannimani R, Perumal A, Krishna SB, Muthusamy SK, Mishra A, Govender P (2014) Digest J Nanomat Biostruct 9:1669
- Prasad R (2014) J Nanoparticles 2014:1. Article ID 963961
- Yang N, Li W-H (2013) Industr Crops Prod 48:81
- Nisha SN, Ayesha OS, Rahaman JSN, Kumar PV, Valli S, Nirmala P, Reena A (2014) Spectrochim Acta Part A 124:194
- Basavegowda N, Lee YR (2013) Mater Lett 109:31
- Velmurugan P, Anbalagan K, Manosathyadevan M, Lee K-J, Cho M, Lee SM, Park JH, Oh SG, Bang KS, Oh BT (2014) Bioprocess Biosyst Eng 37(10):1935–1943
- Kannan RR, Arumugam R, Ramya D, Manivannan K, Anantharaman P (2013) Appl Nanosci 3:229
- Ghosh S, Patil S, Ahire M, Kitture R, Gurav DD, Jabgunde AM, Kale S, Pardesi K, Shinde V, Bellare J, Dhavale DD, Chopade BA (2012) J Nanobiotechnol 10:1
- Das RK, Gogoi N, Bora U (2011) Bioprocess Biosyst Eng 34:615

20. Nagaraj B, Malakar B, Divya TK, Krishnamurthy NB, Liny P, Dinesh R, Iconaru SL, Ciobanu CS (2012) *Digest J Nanomater Biostruct* 7:1289
21. Rajesh WR, Jaya RL, Niranjana SK, Vijay DM, Sahebrao BK (2009) *Curr Nanosci* 5:117
22. Jayaseelan C, Ramkumar R, Rahuman AA, Perumal P (2013) *Industr Crops Prod* 45:423
23. Yallappa S, Manjanna J, Peethambar SK, Rajeshwara AN, Satyanarayan ND (2013) *J Clust Sci* 24:1081
24. Baumann M, Baxendale R (2013) *Beilstein J Org Chem* 9:2265
25. Lauria A, Delisi R, Mingoia F, Terenzi A, Martorana A, Barone G, Almerica AM (2014) *Eur J Org Chem* 2014:3289
26. Dai ZC, Chen YF, Zhang M, Li SK, Yang TT, Shen L, Wang JX, Qian SS, Zhu HL, Ye YH (2015) *Org Biomol Chem* 13:477
27. Ferreira MLG, Pinheiro LCS, Santos-Filho OA, Pecanha MDS, Sacramento CQ, Machado V, Ferreira VF, Souza TML, Boechat N (2014) *Med Chem Res* 23:1501
28. Quahrouch A, Iqhachane H, Taourite M, Engels JW, Sedra MH, Lazrek HB (2014) *Arch Pharm* 347:748
29. Ashwin N, Garg M, Mohan CD, Fuchs JE, Rangappa S, Anusha S, Swaroop TR, Rakesh KS, Kanojia D, Madan V, Bender A, Koefler HP, Basappa Rangappa KS (2015) *Biorg Med Chem* 23:6157
30. Li J, Zheng M, Tang W, He P, Zhu W, Li T, Auo J, Liu H, Jiang H (2006) *Bioorg Med Chem Lett* 16:5009
31. Cho JH, Bernard DL, Sidwell RW, Kern ER, Chu CK (2006) *J Med Chem* 49:1140
32. Xia Y, Liu Y, Wan J, Wang M, Rocchi P, Qu F, Iovanna JL, Peng L (2009) *J Med Chem* 52:6083
33. Pokhodylo N, Shyyka O, Matyichuk V (2013) *Sci Pharm* 81:663
34. Lu J, Ma E, Liu YH, Li YM, Mo L, Zhang ZH (2015) *RSC Adv* 5:59167
35. Belskaya N, Subbotina J, Lesogorova S (2015) *Top Heterocycl Chem* 40:51
36. Hemmaragala NM, Arvidsson PI, Maguire GE, Kruger HG, Govender T (2012) *J Nanosci Nanotechnol* 12:2179
37. Hemmaragala NM, Krause RWM (2014) *Adv Sci Eng Med* 6:612
38. Archer RH (2000) *Anacardiaceae*. In: Leistner OA (ed) *Seed plants of Southern Africa*. Strelitzia 10. National Botanical Institute, Pretoria, pp 56–59
39. Mosa RA, Oyedeji AO, Shode FO, Singh M, Opoku AR (2011) *Afr J Pharm Pharmacol* 5:2698